The Journal of Engineering Research (TJER) Vol. 12, No. 2 (2015) 60-67

Drag Reduction Properties of Nanofluids in Microchannels

H.A. Abdulbari* and F.L.W. Ming

Centre of Excellence for Advanced Research in Fluid Flow; Faculty of Chemical Engineering and Natural Resources, Universiti Malaysia Pahang, Gambang 26300, Kuantan, Pahang, Malaysia.

Received 21 November 2014; Accepted 1 July 2015

Abstract: An experimental investigation of the drag reduction (DR) individualities in different sized micro channels was carried out with nanopowder additives (NAs) (bismuth(III) oxide, iron(II/III) oxide, silica, and titanium(IV) oxide) water suspensions/fluids. The primary objective was to evaluate the effects of various concentrations of NAs with different microchannel sizes (50, 100, and 200 µm) on the pressure drop of a system in a single phase. A critical concentration was observed with all the NAs, above which increasing the concentration was not effective. Based on the experimental results, the optimum DR percentages were calculated. The optimum percentages were found to be as follows: bismuth III oxides: ~65% DR, 200 ppm and a microchannel size of 100 µm; iron II/III oxides: ~57% DR, 300 ppm, and a microchannel size of 50 µm; titanium IV oxides: ~57% DR, 200 ppm, and a microchannel size of 50 µm, and silica: 55% DR, 200 ppm, and a microchannel size of 50 µm.

Keywords: Microchannels, Pressure drop, Drag reduction, Nanopowder additives.

خواص المقاومة الهيدروليكية للموائع النانوية في القنوات الميكروية الصغيرة

حيدر أ عبدالباري، وفيونا لنك وانك منك

المستخلص: تم في هذا البحث المعملي دراسة مجموع السمات المميزة لانخفاض المقاومة الهيدروليكية في مختلف القنوات الميكروية الصغيرة الحجم وذلك باستخدام إضافات مسحوق نانو البودر (مركب أكسيد البزموت الثالث، وأكسيد الحديد الثنائي/ الثلاثي، والسليكا، وأكسيد التيتانيوم الرباعي) مع عوالق الماء/الموائع. وكان الهدف الأساسي تقييم تأثير التراكيز المختلفة لإضافات مسحوق نانو البودر مع القنوات الميكروية ذات الأطوال المختلفة (50 مايكرومتر، 100 مايكرومتر، 200 مايكرومتر) على هبوط الضغط في نظام أحادي الطور. ولوحظ وجود تركيز حرج مع جميع التراكيز المختلفة لإضافات مسحوق نانو البودر، بحيث ان استخدام تراكيز أعلى من ذلك التركيز الحرج أثبت عدم جدواه. وبناءً على النتائج المختبرية، تم حساب النسب المئوية المثلى لإضافات مسحوق نانو البودر مع الأطوال المختلفة للقنوات الميكروية، حيث كانت لمركب أكسيد البزموت الثالث: 65٪ مسحوق نانو البودر، 200 جزء في المليون، 100 مايكرومتر؛ وكانت لأكسيد الحديد الثنائي/ الثلاثي: 57٪ مسحوق نانو البودر، 300 جزء في المليون، 50 مايكرومتر؛ بينما كانت لأكسيد التيتانيوم الرباعي: 57٪ مسحوق نانو البودر، 200 جزء في المليون، 50 مايكرومتر؛ وكانت للسليكا: 55٪ مسحوق نانو البودر، 200 جزء في المليون، 50 مايكرومتر.

الكلمات المفتاحية: القنوات الميكروية الصغيرة، هبوط الضغط، المقاومة الهيدروليكية، إضافات مسحوق نانو البودر

*Corresponding authors' e-mail: hayder.bari@gmail.com

1. Introduction

The study of drag reduction (DR) in microchannels has raised considerable interest in researchers all over the world. DR additives (DRAs), such as polymers, surfactants, and microbubbles, have proven their effectiveness and are appreciated by many industries for their economic value (Nghe *et al*. 2010).

The use of diverse polymers such as DRAs has been reported previously (Abubakar *et al*. 2014; Al-Sarkhi 2012; Matras and Kopiczak 2015; Edomwonyi-Outu, Chinaud and Angeli 2015; Hong *et al*. 2015; Iaccarino *et al*. 2010; Resende *et al*. 2011) and surfactants (Drzazga *et al*. 2013; Li *et al*. 2008; Różański 2011; Yu and Kawaguchi 2006; Tuan Mizunuma 2013; Qi *et al*. 2011) depending upon the polarities and different behaviors in a turbulent flow (Tarn and Pamme 2014), while the impact of other colloidal suspensions, such as nanofluids, in reducing the pressure drop has not been widely studied. The dispersion quality of the nanoparticles in the base fluid and the stability of the suspension play a crucial role in most applications of practical interest (Rivet *et al*. 2011; Xie *et al*. 2003; Choi *et al*. 2007; Ganguly *et al*. 2009). Zhao *et al*. (2009) studied the viscosity of silicon dioxide nanofluids with different particle sizes and pH values. The results revealed that the nanoparticle diameter is of crucial importance to the viscosity of a nanofluid. The smaller the nanoparticles, the larger the viscosity and the greater the dependence on the nanofluid volume fraction. Zhao *et al*. (2009) studied the effect of silica-based nanofluids as DRAs. The results suggested that the DR enhanced increasing nanofluid concentrations up to a critical concentration, above which no significant DR was observed. Pouranfard. (2014) observed an increase in the viscosity of a fluid with increasing concentrations of nanofluid DRAs and decreases in temperature. Kostic (2013) reported a comparative study of silica and carbon nanotubes (CNTs), where the CNTs were found to be better DRAs (75%) than silica with a maximum reduction of 60% (Yang *et al*. 2005).

Very few studies have been done on DR using nanoparticles compared to polymers and surfactants. Therefore, in this study, nanofluids at different operating conditions were injected through microchannels, and the effects of different parameters on DR were investigated. Pressure drop was calculated as a function of flow rate (rpm) in different sized microchannels (50, 100, and 200 μm) by varying the concentration of different types of oxide nanoparticles, including bismuth, iron, silica, and titanium. The pressure drop was later applied in calculating the DR efficacy (%DR) of a particular nanofluid. In addition, the effect of flow rate and channel size on DR was also investigated.

2. Experimental Procedure

2.1 *Materials*

Bismuth(III) oxide, iron(II, III) oxide, titanium (IV) oxide, and silicon(II) oxide were purchased from Sigma-Aldrich (St. Louis. Missouri, USA) and used without any alterations [Table 1]. Deionized water was used to prepare samples and make dilutions.

Table 1. Physical properties of nanoparticles used.

Working fluids	M. weight (g/mol)	Size	Density (g/mL)
Bismuth(III) oxide (Bi_2O_3)	465.96	90–210	0.5–1.1
Iron(II,III) oxide (Fe_3O_4)	251.53	50–100	4.8–5.1
Silica (SiO_2)	60.08	200–300	0.037
Titanium(IV) oxide (TiO_2)	79.87	<100	--

2.2 *Nanofluid Solution Preparation*

Nanoparticle solutions were prepared in deionized water for each oxide at five different concentrations, ranging from 100–500 ppm. The fluids were homogenized at high speed for 10 minutes with a stirrer and then left overnight on low speed to achieve maximum dispersion. Before running each experiment, the solution was stirred for two hours at 100 rpm to avoid any agglomeration.

2.3 *Experimental Setup*

Straight microchannels of 50, 100, and 200 μm with a length of 58.5 mm (TOPAS Advanced Polymers, Frankfurt-Höchst, Germany) were employed in this study. The solution was transferred through two syringes via a syringe pump (model SN-50F6) connected to a T-junction connection whose outlet was connected to another T-junction connection. A pressure transmitter (model: STK336) and the inlet of the microchannel were connected to the outlet of the second T-junction connection. The solutions were pumped into the microchannel via connecting tubes.

The flow rate of the solutions was controlled using the syringe pump. The flow of the liquid in the microchannel was observed using an HBO 50 microscope (Zeiss International, Oberkochen, Germany) connected to a camera. The pressure drop across the microchannel was observed using the pressure transmitter and the results were recorded. The %DR was calculated using Eqn. 1.

$$\%\mathrm{DR} = \frac{\Delta P_b - \Delta P_a}{\Delta P_b} \times 100 \qquad (1)$$

Where,

ΔP_b = pressure drop before adding DRA

ΔP_a = pressure drop after adding DRA

3. Results and Discussion

A series of experiments were performed to study the effects of nanofluid concentration, microchannel size, and flow rate on pressure drop and %DR. It was found that the %DR rises with increasing nanofluid concentration. However, there is a critical concentration above which no more reduction can be attained. In the present study, the critical concentration obtained was almost the same for all oxide nanoparticles (200 ppm) with the exception of Fe_3O_4 (300 ppm) [Table 2].

Figure 1 presents a comparison of the pressure drop at the critical concentrations of nanofluids and deionized water versus the flow rate in the microchannels. A regular pressure drop trend was observed with an increasing flow rate in all cases. Increasing the flow rate increases the degree of turbulence which provides a better platform for DRAs to perform (Stone and Ajdari 2014). SiO_2 showed a maximum pressure drop at its critical concentration, which may be due to the fact that the mechanism of DR by SiO_2 nanoparticles is mainly a surface modification. The SiO_2 nanoparticles have good rigidity and reduce the friction factor through dispersion into the liquid phase and contact with the pipe surface, so a higher pressure drop was observed (Zhao *et al.* 2009).

Figures 2–5 show the %DR versus the rate of flow in the different sized microchannels and at different oxide nanoparticle concentrations. The DR is greater with smaller particles as the smaller sized particles with larger surface areas result in the migration effect, where a bond is formed between the transporting fluid molecules and the DR agents (Khadom and Abdul-Hadi 2014). It was observed that the use of nanofluids at low concentrations did not cause a serious reduction in the pressure drop which is due to the small size of the nanoparticles (Abdulbari, Shabirin and Abdurrahman 2013).

The diameter of the microchannels does not seem to affect the %DR greatly in contrast to the behavior usually observed with a reduction in diameter (Lee and Mudawar 2007). The effect of solution velocity (m) on the %DR was studied in terms of the volumetric flow rate. The results show that the %DR increases with increasing fluid velocity. Increasing the fluid velocity means increasing the degree of turbulence inside the pipe, which will provide a better medium for the drag reducer to be more effective (Byrne, Hart and da Silva 2012).

Figure 2 presents the %DR while keeping the concentration constant for all the nanofluids at 100 ppm with varying microchannel sizes (50, 100, and 200 μm). An increase in %DR was observed when increasing the microchannels' sizes from 50 to 200 μm. This can be explained by the presence of large

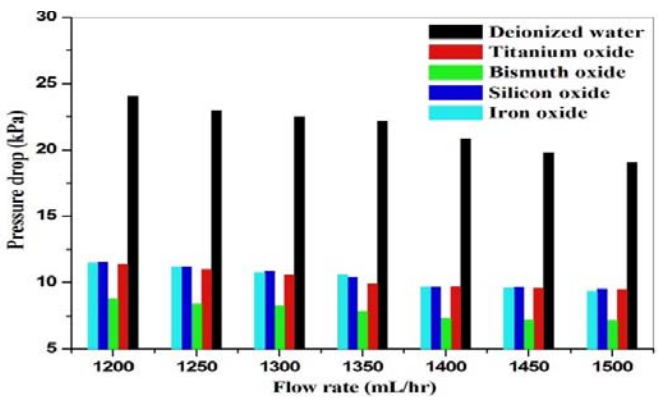

Figure 1. A comparative study of pressure drop between deionized water and oxides used in the study.

Table 2. Parameters affecting the drag reduction in different nanofluids.

Oxide	Channel size	Critical Con.	Flow rate	Pressure drop	Drag reduction
	µm	ppm	ml/hr	kPa	%
Titanium	50	200	1350	9.93	56.9
	100	200	1250	10.74	53.3
	200	200	1350	9.34	51.3
Bismuth	50	200	1400	8.28	63.0
	100	200	1400	7.35	64.8
	200	200	1200	8.67	57.5
Silicon	50	200	1350	10.35	55.1
	100	200	1400	9.99	52.1
	200	200	1400	9.68	57.6
Iron	50	300	1450	9.59	56.8
	100	300	1350	9.66	56.5
	200	300	1350	9.94	48.2

µm = micrometer; Con. = concentration; ppm = parts per million; kPa = kilopascals

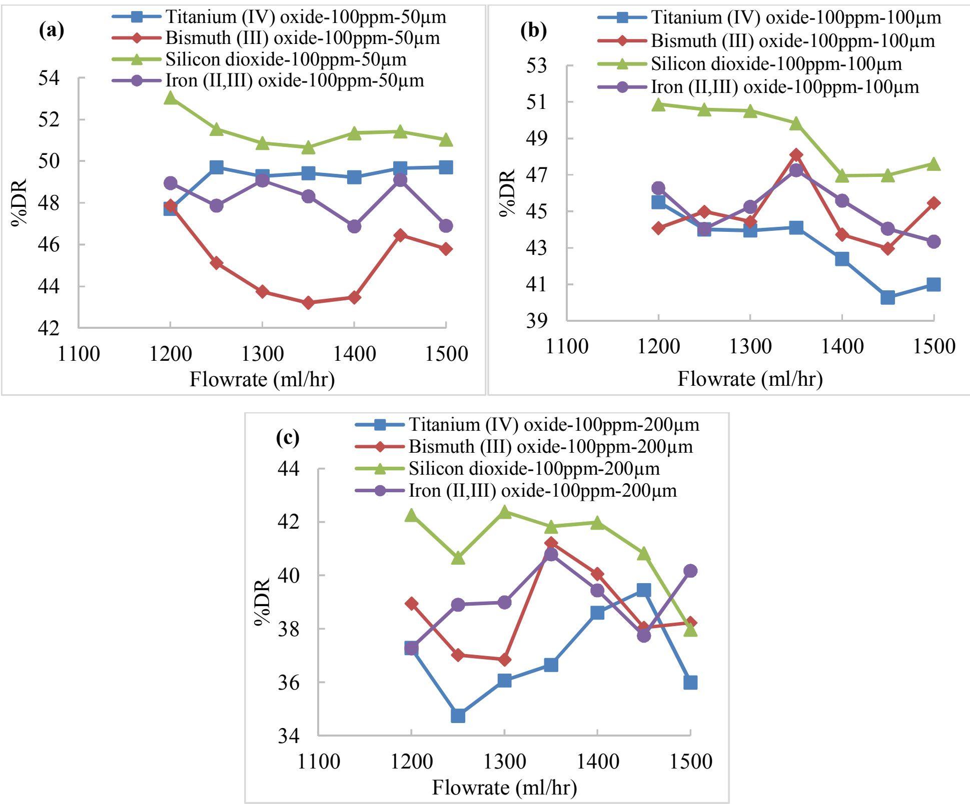

Figure 2. Variations of %DR with a nanofluid concentration of 100 ppm.

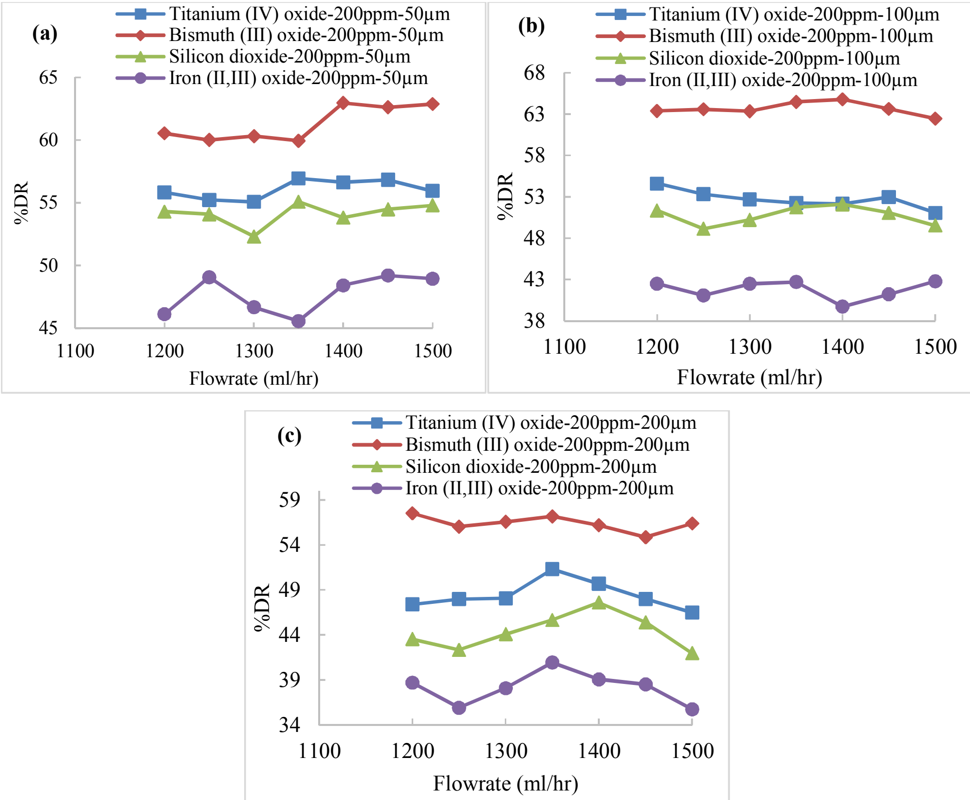

Figure 3. Variations of %DR with nanofluid concentration of 200 ppm.

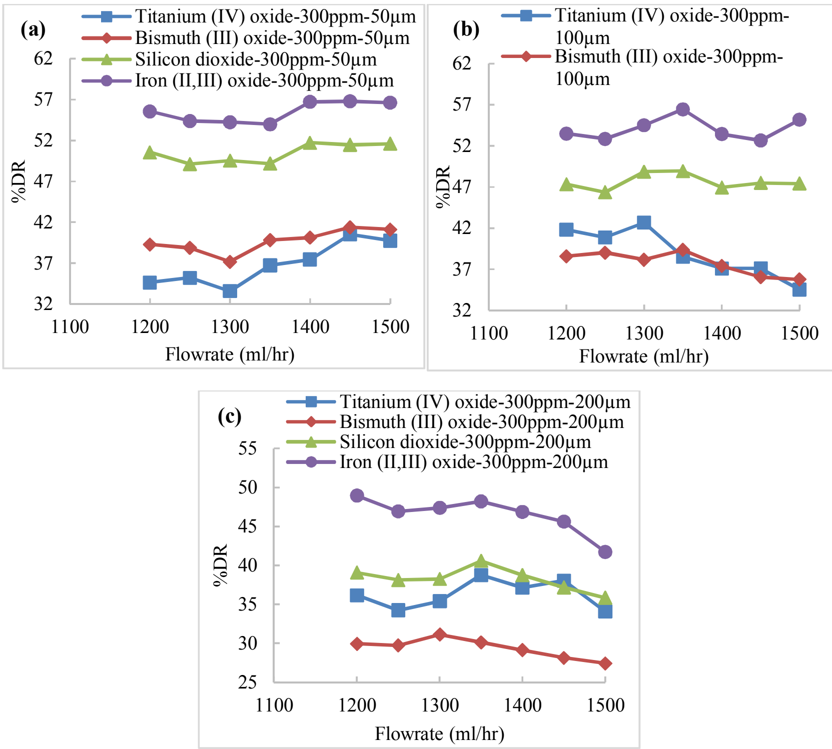

Figure 4. Variation in %DR at a nanofluid concentration of 300 ppm.

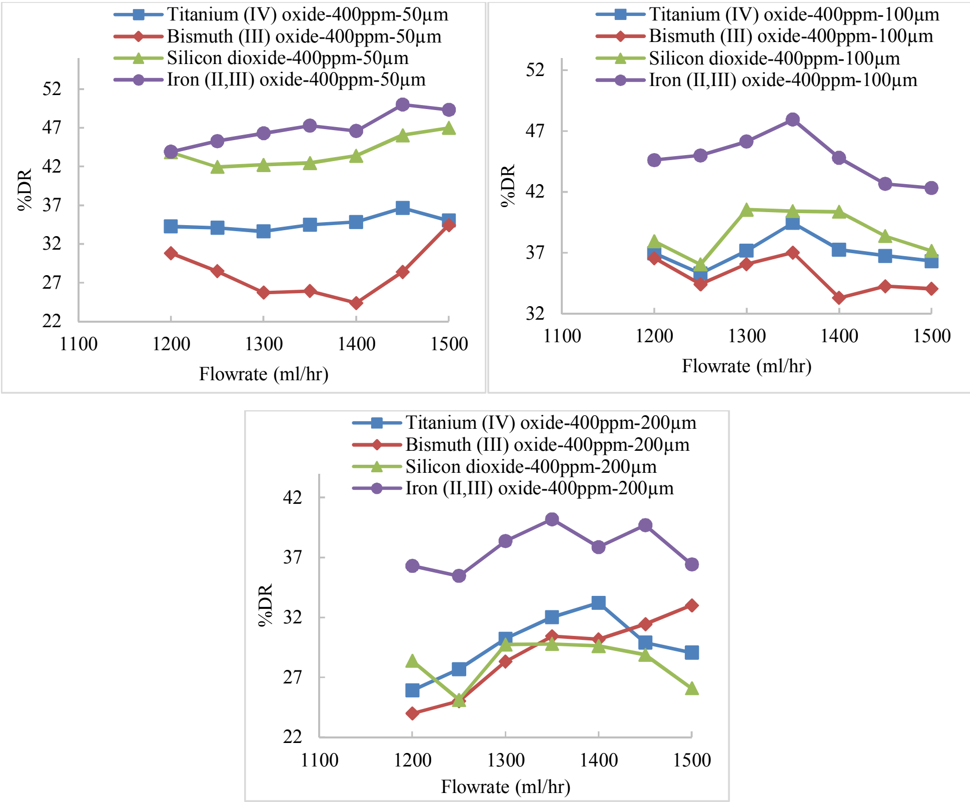

Figure 5. Variations in %DR at nanofluid concentrations of 400 ppm.

eddies in the larger microchannels which absorb a large amount of energy from the flow. In smaller microchannels, more smaller eddies are formed, but some small eddies are unable to absorb enough energy and are incapable of overcoming the viscosity resistance (Kim *et al*. 2000; Khadom and Abdul-Hadi 2014; Al-Sarkhi and Hanratty 2001). SiO_2 exhibited the highest %DR of all the microchannels, which may be due to the larger sized silica particles settling down quickly and further decreasing the diameter of the microchannels.

Figure 3 depicts the maximum DR achieved in all the oxides except for Fe_3O_4 nanofluids at a concentration of 200 ppm, which is a clear indication of reaching a critical concentration. Bi_2O_3 exhibited the highest %DR (~65%) at the critical concentration with a microchannel size of 100 µm at 1400 rpm, which reduced to 200 µm-sized microchannels (~58%) with a flow rate of 1200 rpm. In the case of SiO_2 and TiO_2, the maximum drag achieved at the critical concentration was ~57.5 and ~57% with 200 and 50 µm-sized microchannels, respectively.

The iron oxide nanofluid exhibited maximum DR at a concentration of 300 ppm in all the microchannels [Fig. 4]. Maximum DR (~ 56.8 %) was achieved with 50 µm-sized microchannels and a flow rate of 1400 mL/hr. In cases of 100 µm-sized microchannels, a nearly identical increasing trend was observed and maximum drag reduction (~56.5 %) was observed at a slightly lower flow rate (1350 mL/hr). A decreasing trend in drag was observed for all the other oxides, which confirmed that all the oxides had reached their critical concentration limit; increasing the concentration further had no more effect on the pressure drop in a flow.

A gradual decrease in the DR properties of the iron oxide nanofluid was observed at 400 ppm [Fig. 5], emphasizing that iron oxide nanofluids are more effective in the concentration range of 300–400 ppm.

All the other nanofluids exhibited a very low DR; thus, it is obvious that, after a critical limit has been reached, increasing the concentration has no positive effect on DR efficiency and a negative impact on the flow of a system.

4. Conclusions

To conclude, the DR performances of different nanofluids were studied at diverse concentrations in different sized microchannels. It was observed that all the nanofluids exhibited a certain critical concentration above which increasing the concentration had no greater impact on the pressure drop or the DR of the system. Increasing the flow rate also had an impact on DR efficiency, but it was noticed that, above the critical concentration limit, the flow rate did not have much effect on the %DR. The channel size was found to have no effect on the DR efficiency of the nanofluids.

Acknowledgments

Authors are grateful to Universiti Malaysia Pahang, for financial assistance.

References

Abubakar A, Al-Wahaibi T, Al-Wahaibi Y, Al-Hashmi AR, Al-Ajmi A (2014), Roles of drag reducing polymers in single- and multi-phase flows. *Chemical Engineering Research and Design* 92(11): 2153–2181.

Al-Sarkhi A (2012), Effect of mixing on frictional loss reduction by drag reducing polymer in annular horizontal two-phase flows. *International Journal of Multiphase Flow* 39: 186–192.

Al-Sarkhi A, Hanratty TJ (2001), Effect of pipe diameter on the performance of drag-reducing polymers in annular gas-liquid flows. *Chemical Engineering Research and Design* 79(4): 402–408.

Byrne M, Hart R, da Silva A (2012), Experimental thermal hydraulic evaluation of CuO nanofluids in microchannels at various concentrations with and without suspension enhancers. *International Journal Heat Mass Transfer* 55: 2684–2691.

Choi CS, Park SJ, Choi HJ (2007), Carbon nanotube/polyaniline nanocomposites and their electrorhelogical characteristics under an applied electric field. *Current Applications in Physics* 7: 352–355.

Drzazga M, Gierczycki A, Dzido G, Lemanowicz M (2013), Influence of nonionic surfactant addition on drag reduction of water based nanofluid in a small diameter pipe. *Chinese Journal of Chemical Engineering* 21(1): 104–108.

Edomwonyi-Otu LC, Chinaud M, Angeli P (2015), Effect of drag reducing polymer on horizontal liquid–liquid flows. *Experimental Thermal and Fluid Science* 64: 164–174.

Ganguly S, Sikdar S, Basu S (2009), Experimental investigation of the effective electrical conductivity of aluminum oxide nanofluids. *Powder Technology* 196: 326–330.

Hong C, Choi HJ, Zhang K, Renou F, Grisel M (2015), Effect of salt on turbulent drag reduction of xanthan gum. *Carbohydrate Polymers* 121: 342–347.

Iaccarino G, Shaqfeh ESG, Dubief Y (2010), Reynolds-averaged modeling of polymer drag reduction in turbulent flows. *Journal of Non-Newtonian Fluid Mechanics* 165(7–8): 376–384.

Khadom AA, Abdul-Hadi AA (2014), Performance of polyacrylamide as drag reduction polymer of crude petroleum flow. *Ain Shams Engineering Journal* 5(3): 861–865.

Kim NJ, Lee JY, Yoon SM, Kim CB, Hur BK (2000), Drag reduction rates and degradation effects on synthetic polymer solution with surfactant additives. *Journal of Industrial and Engineering Chemistry* 6: 412–418.

Kostic MM (2013), Friction and heat transfer characteristics of silica and CNT nanofluids in a tube flow. Proceedings of the 8th Annual International *Conference on Energy and Environment*, Rhodes Island, Greece.

Lee J, Mudawar I (2007), Assessment of the effectiveness of nanofluids for single phase and two-phase heat transfer in micro-channels. *International Journal of Heat Mass Transfer* 50(3-4): 452–463.

Li FC, Kawaguchi Y, Yu B, Wei JJ, Hishida K (2008), Experimental study of drag-reduction mechanism for a dilute surfactant solution flow. *International Journal of Heat and Mass Transfer* 51(3–4): 835–843.

Matras Z, Kopiczak B (2015), Intensification of drag reduction effect by simultaneous addition of surfactant and high molecular polymer into the solvent. *Chemical Engineering Research and Design* 96: 35–42.

Nghe P, Tabeling P, Ajdari A (2010), Flow-induced polymer degradation probed by a high throughput microfluidic set-up. *Journal of Non-Newtonian Fluid Mechanics* 165(7–8): 313–322.

Pouranfard AR, Mowla D, Esmaeilzadeh F (2014), An experimental study of drag reduction by nanofluids through horizontal pipe turbulent flow of a Newtonian liquid. *Journal of Industrial and Engineering Chemistry* 20(2): 633–637.

Qi Y, Kesselman E, Hart DJ, Talmon Y, Mateo A, Zakina JL (2011), Comparison of oleyl and elaidyl isomer surfactant–counterion systems in drag reduction, rheological properties and nanostructure. *Journal of Colloid and Interface Science* 354(2): 691–699.

Resende PR, Kim K, Younis BA, Sureshkumar R, Pinhoa RT (2011), A FENE-P k–ε turbulence model for low and intermediate regimes of polymer-induced drag reduction. *Journal of Non-Newtonian Fluid Mechanics* 166(12–13): 639–660.

Rivet C, Hirsch A, Hamilton S, Lu H (2011), Microfluidics for Medical Diagnostics and Biosensors. *Chemical Engineering Science* 66: 1490–1507.

Różański J (2011), Flow of drag-reducing surfactant solutions in rough pipes. *Journal of Non-Newtonian Fluid Mechanics* 166(5–6): 279–288.

Stone HA, Ajdari A (2004), Engineering flows In small devices: Microfluidics Toward A Lab-On-A-Chip. *Annual Review of Fluid Mechanics* 36: 381–411.

Tarn, MD, Pamme N (2014), *Microfluidics*, in *Reference Module in Chemistry, Molecular Sciences and Chemical Engineering* Elsevier.

Tuan NA, Mizunuma H (2013), High-shear drag reduction of surfactant solutions. *Journal of Non-Newtonian Fluid Mechanics* 198: 71–77.

Xie H, Lee H, Youn W, Choi M (2003), Nanofluids containing multi walled carbon nanotubes and their enhanced thermal conductivities. *Journal of Applied Physics* 94: 4967–4972.

Yang Y, Zhang Z, Grulke EA, Anderson WB, Wu G (2005), Heat transfer properties of nanoparticle-in-fluid dispersions (nanofluids) in laminar flow. *International Journal of Heat Mass Transfer* 48(6): 1107–1116.

Yu B, Kawaguchi Y (2006), Parametric study of surfactant-induced drag-reduction by DNS. *International Journal of Heat and Fluid Flow* 27(5): 887–894.

Zhao JF, Luo ZY, Ni MJ, Cen KF (2009), Dependence of nanofluid viscosity on particle size and pH value. *Chinese Physics Letters* 26: 066202.